MODIS Semi-annual Report (January 2003 – June 2003)

Bo-Cai Gao, Po Li, Pui King Chan, and Ping Yang

(This reports covers the MODIS **cirrus characterization and correction** algorithm and the MODIS **near-IR water vapor algorithm**)

Main topics addressed in this time period:

1. **MODIS near-IR water vapor algorithm**:

During this reporting period, our main activities on MODIS near-IR water vapor algorithm include: (a) evaluation of near-IR water vapor data products produced with the recent Collection 4 softwares, (b) additional validation of MODIS near-IR water vapor retrievals using ground-based instruments, (c) preliminary work on combining the monthly-mean MODIS near-IR water vapor products over land and the SSMI water vapor products over ocean to form a high quality water vapor data set for climate studies, and (d) revision of a paper on MODIS near-IR water vapor algorithm.

(a) We made extensive and time-consuming analysis of the near-IR water vapor data products produced with the Collection 4 softwares and to make sure that there are no obvious errors in our data products.

(b) We studied the work of British scientists at the Department of Geomatic Engineering, University College London on comparing precipitable water vapor obtained from radiosondes, GPS, and MODIS measurements over Germany. There is a dense GPS network with more than 100 sites all over Germany. It is possible to retrieve water vapor amount on a slant path
from GPS data based on the differences between "wet" delays and "dry" delays. We feel that the GPS measurements can have important contributions to the validation of MODIS near-IR water vapor data products. However, serious issues remain. For examples, the view zenith angles between MODIS and GPS are very different. MODIS' view zenith angles are all less than 65 degrees, while the GPS view zenith angles are all greater than 65 degrees. In an approximate sense, MODIS has a "nadir" viewing geometry, while a GPS instrument has a "horizontal" viewing geometry. The two types of instruments will not be able to view the same atmosphere simultaneously. Each GPS station requires independent calibrations. The water vapor images obtained from a GPS network may not be internally consistent, because the calibration errors for different GPS stations in the network can be different. On the other hand, MODIS

near-IR water vapor images can be internally more consistent, because only one instrument and one set of near-IR channels are used in the water vapor derivations for the whole image.

(c) We have conducted preliminary work on combining the monthly-mean MODIS near-IR water vapor products over land and the SSMI water vapor products over ocean to form a high quality water vapor data set for climate studies. The retrieval of water vapor from MODIS near-IR channels requires measurements over reflective targets, such as clear land surfaces, clouds, or oceanic areas with extended sunglint patterns. Over the dark ocean surfaces, our Level-2 water vapor values are not as good as those over bright land surfaces. As a result, we do not generate the Level-3 monthly-mean near-IR water vapor images over dark oceans. The upper left plot in Figure 1 shows a monthly-mean MODIS near-IR water vapor image for July 2001. Nice water

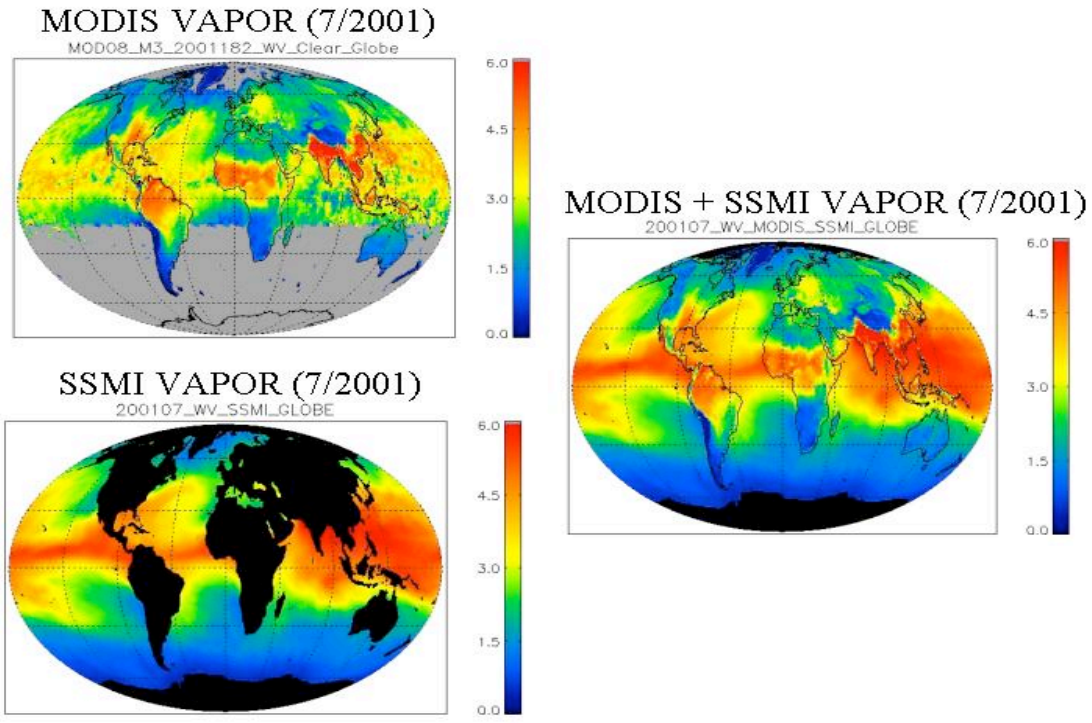

Fig. 1. A monthly-mean MODIS near-IR water vapor image (upper left) for July 2001, a monthly-mean SSMI water vapor image (lower left) for the same month, and a MODIS-SSMI-combined water vapor image (right).

vapor distributions over the northern hemisphere are observed. For examples, very small amounts of water vapor are observed over the Sahara desert in northern Africa, the Himalayan Mountains in Asia, and Andes Mountains in South America. The Indian Continent and Indo-China regions are saturated with water vapor. Due to the lack of reflective ocean surface (sun glint) in this month, the near-IR water vapor products are not generated over major portions of oceanic areas (masked as the 'grey' areas in this plot) in the southern hemisphere.

The column water vapor amount, also known as the total precipitable water (TPW), has been retrieved over oceans from passive microwave sensors dating back to the Nimbus series of experimental instruments. There are several algorithms using measurements near the center of a weak water vapor absorption line at 22 GHz for the retrieval of oceanic TPWs. Currently there are at least three Special Sensor Microwave Imagers (SSMIs) or similar sensors on board different spacecrafts for operational retrieval of TPWs over oceans. The plot in the lower left portion of Fig. 1 shows a monthly-mean SSMI water vapor image for July 2001. Nice water vapor distributions over oceanic areas are observed. Retrievals of TPWs over land at the microwave frequency are not possible due to the high emissivity over most land surfaces (~0.95) as compared to clear ocean (~0.5). As a result, the land areas are masked as "black" in this plot.

The plot in the right portion of Fig. 1 shows a global water vapor image for the same month by combining the MODIS near-IR water vapor product over land and the SSMI water vapor product over the ocean. From this image, it is seen that the water vapor values over the land-water boundary areas are smoothly connected, which indicates that the systematic errors between the two types of water vapor products are very small. Through such combinations, a water vapor data set with superior quality and simultaneous land and ocean coverages is produced. Such combined water vapor data products can have important applications in climate related research.

(d) During this time period, we made revision to a manuscript describing the MODIS near-IR water vapor algorithm and presenting sample results. This manuscript was published by the Journal of Geophysics Research – Atmosphere in July 2003.

2. **MODIS cirrus reflectance algorithms**:

During this time period, our main activities on MODIS cirrus reflectance

algorithm include: (a) evaluation of cirrus reflectance products generated with the Collection 4 softwares, (b) examination of seasonal and global distributions of cirrus clouds associated with the 2002 El Nino event, (c) examination of thin cirrus contaminations in sea surface temperature products retrieved from IR emission channels, and (d) publication of papers on cirrus clouds observed with MODIS.

(*a*) We made extensive analysis of cirrus reflectance data products generated with the Collection 4 softwares. Radiometric calibration for the MODIS 1.375-micron channel (Ch. 26) was improved significantly. The well-known cross-talking problem associated with this channel was largely removed using an empirical algorithm developed by Mr. Chris Moeller of University of Wisconsin. Figure 2a shows an example of cirrus reflectance image produced with an earlier version of softwares. Many lines are seen in this image. Figure 2b shows the cirrus reflectance image for the same area but produced with the Collection 4 softwares. The new image looks much smoother.

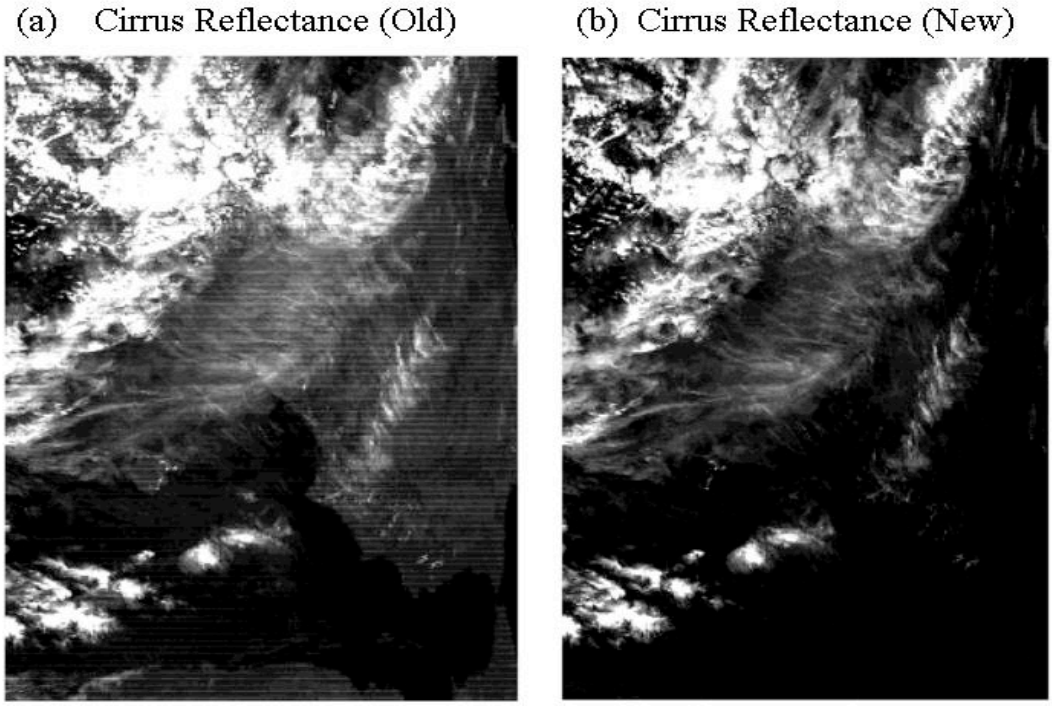

Fig. 2. (a) – a cirus reflectance image produced with old softwares, and (b) – the corresponding cirrus reflectance images produced with the Collection 4 softwares.

Through careful analysis of the cirrus reflectance data products over different geographical regions, we found that the cross-talking problem was slightly "over-corrected" over the Pacific Ocean and west to the South America. The MODIS Calibration and Support Team is going to further improve the algorithm for removing the cross-talking effect by including Channel 25 in the L1B calibration equation for

Channel 26 in the future.

(***b***) We made preliminary studies of seasonal and global distributions of cirrus clouds associated with the 2002 El Nino event. Figures 3a – 3c show sample

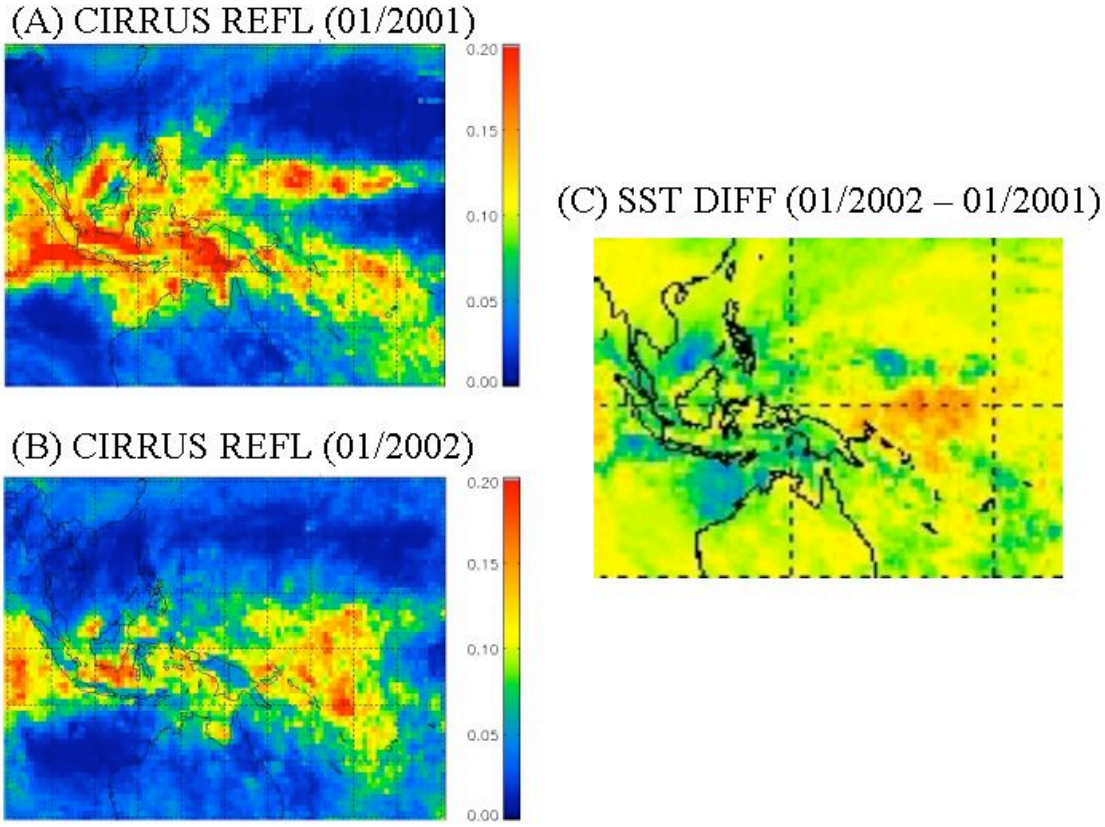

Fig. 3. MODIS cirrus reflectance images covering the latitude range of 30°N – 30°S and a longitude range of 90°E – 170°W for January 2001 (a), January 2002 (b), and the reflectance difference image (01/2002 – 01/2001) (c).

results. In Fig. 3a we show a cirrus reflectance image (around the "warm pool" in the Pacific Ocean) covering the latitude range of 30°N – 30°S and a longitude range of 90°E – 170°W for January 2001. Fig. 3b is similar to Fig. 3a except for January 2002. Fig. 3c is the cirrus reflectance difference image (01/2002 – 01/2001). The color bar is not shown in Fig. 3c, but the color coding is made in such a way that blue corresponds to a reflectance difference of –0.2, and red +0.2. It is obvious to see from the Fig. 3a and 3b images that, in January 2002, the reflectances of cirrus clouds over Indonesia decreased while that over areas east of Indonesia increased in comparison with the January 2001 cirrus reflectance image. This can also be seen from the Fig. 3c difference image. The changes in cirrus reflectance patterns can be attributed to the eastward movement of "warm pool" during the El Nino year.

(***c***) Cirrus clouds are widely distributed around the globe. At any given moment, more than 50% of the area is covered by cirrus clouds based on our observations with the 1.375-micron MODIS channel. At present, many land, ocean, and atmospheric products are derived from MODIS data without any mechanisms for removing contaminations from thin cirrus clouds. We think that there are now great needs for assessing the cirrus-contamination problems for many standard MODIS data products. Here we would like to show examples of cirrus contaminations on the IR sea surface temperature data products.

We show in Figure 4a an IR SST temperature image downloaded from the MODIS Ocean Group's web site. The image was retrieved with the MODIS SST algorithm from one set of MODIS data acquired over Central America on December 3, 2002 at UTC 2000. Figure 4b shows the cirrus cloud image processed from the MODIS 1.38-micron channel data. This channel is very sensitive in detecting thin cirrus clouds. By comparing Figs. 4a and 4b, it is seen that the SST values are small (blue in Fig 4a image) over areas covered by cirrus clouds. The shapes of the white clouds in Fig. 4b are exactly the same as those blue features in Fig. 4a. This demonstrates clearly that the current MODIS SST algorithm does not properly estimate surface temperatures over areas affected by cirrus clouds. The absorption effects by ice particles in cirrus clouds were directly passed over to the Level 2 SST data products. Although cloud mask is used in the generation of Level 3 MODIS SST data products, pixels slightly contaminated by thin cirrus clouds are inevitably used in the generation of Level 3 global SST data products.

Figure 4c shows a monthly-mean cirrus reflectance image over the globe for December of 2002. These clouds are distributed unevenly at different latitudes and longitudes. For example, a large area (roughly a triangle in the lower left part of this figure) in the Pacific Ocean and west to the Andes Mountains in Fig. 4c has little cirrus clouds, while the areas surrounding the "triangle" have significant amounts of cirrus clouds. Because cirrus clouds cover large portions of the earth's surface areas and because the MODIS SST algorithm does not correct for the cirrus absorption effects, the SST products retrieved from the MODIS data are expected to have variable levels of biases over large areas in different geographical regions.

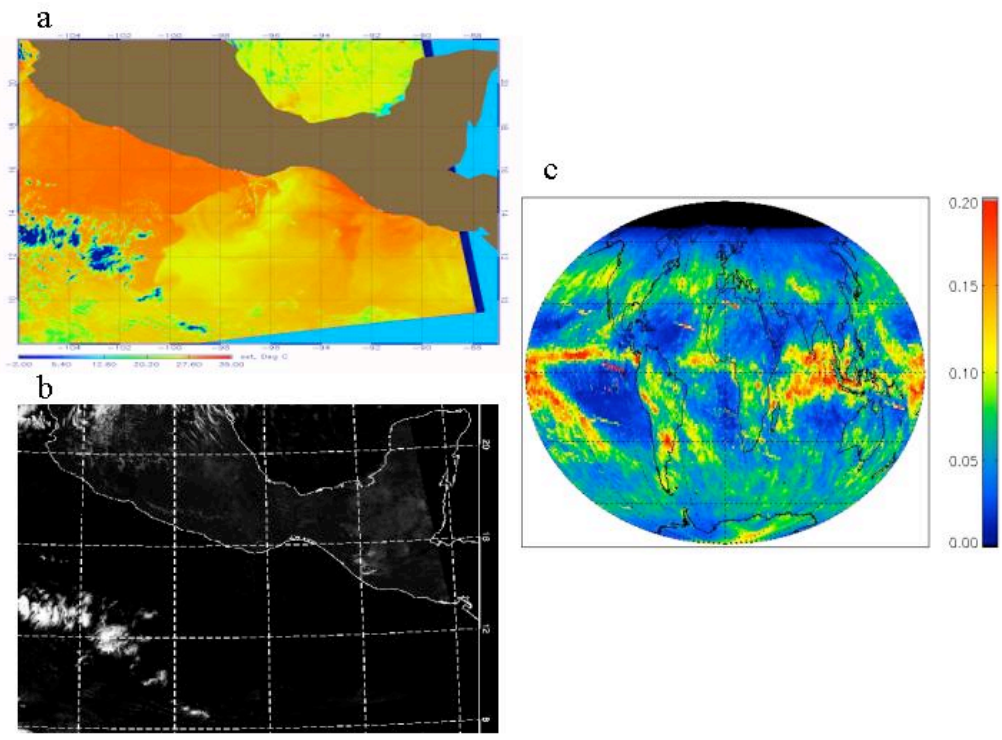

Fig. 4. (a) – a MODIS SST image over Central America; (b) – a cirrus cloud image over the same area; and (c) – a global monthly-mean cirrus image.

(*d*) During this time period, we have several papers published in scientific journals. One paper on detecting polar clouds during the daytime using the MODIS 1.375-micron channel appeared in the special AQUA IEEE issue. Another short paper on measurements of water vapor and high clouds over the Tibetan Plateau with the Terra MODIS instrument was also published by IEEE Transaction on Geoscience and Remote Sensing. One of the figures in this paper was selected for the cover page of IEEE's April 2003 issue (Volume 41, No. 4).

3 **Publications**:

Gao, B.-C., and Y. J. Kaufman, Water vapor retrievals using Moderate Resolution Imaging Spectrometer (MODIS) near-IR channels, J. Geophys. Res., 108, 4389 – 4398, 2003 (doi: 10.1029/2002JD003023).

Gao, B.-C., P. Yang, G. Guo, S. K. Park, W. J. Wiscombe, and B.-D. Chen, Measurements of water vapor and high clouds over the Tibetan Plateau with the Terra MODIS

instrument, IEEE Transa. Geosci. Remote Sensing, 41, 895-900, 2003 (doi: 10.1109/TGRS.2003.810704).

Li, R.-R., Y. J. Kaufman, B.-C. Gao, and C. O. Davis, Remote sensing of suspended sediments and shallow coastal waters, IEEE Trans. Geosci. Remote Sensing, 41, 559-566, 2003 (doi: 10.1109/TGRS.2003.810227).

Gao, B.-C., P. Yang, and R.-R. Li, Detection of high clouds in polar regions during the daytime using the MODIS 1.375-μm channel, IEEE Transa. Geosci. Remote Sens., 41, 474-481, 2003 (doi: 10.1109/TGRS.2002.808290).

King, M. D., W. P. Menzel, Y. J. Kaufman, D. Tanre, B.-C. Gao, S. Platnick, S. A. Ackerman, L. A. Remer, R. Pincus, and P. A. Hubanks, Cloud and aerosol properties, precipitable water, and profiles of temperature and humidity from MODIS, IEEE Trans. Geosci. Remote Sens., 41, 442-458, 2003 (doi: 10.1109/TGRS.2002.808226).

Yang, P., H.-L. Wei, B. A. Baum, H.-L. Huang, A. J. Heymsfield, Y. X. Hu, B.-C. Gao, and D. D. Turner, The spectral signature of mixed-phase clouds composed of non-spherical ice crystals and spherical liquid droplets in the terrestrial window region, J. Quant. Spectros. Radit. Transfer, 79-80, 1171-1188, 2003 (doi: 10.1016/S0022-4073(02)00348-5).